

# Bouncy particle sampler with infinite exchanging parallel tempering

Yohei Saito <sup>\*1</sup>, Shun Kimura<sup>1</sup>, and Koujin Takeda <sup>†2</sup>

<sup>1</sup>Center for Mathematics and Data Science, Gunma University

<sup>2</sup>Graduate School of Science and Engineering, Ibaraki University

## Abstract

Bayesian inference is useful to obtain a predictive distribution with a small generalization error. However, since posterior distributions are rarely evaluated analytically, we employ the variational Bayesian inference or sampling method to approximate posterior distributions. When we obtain samples from a posterior distribution, Hamiltonian Monte Carlo (HMC) has been widely used for the continuous variable part and Markov chain Monte Carlo (MCMC) for the discrete variable part. Another sampling method, the bouncy particle sampler (BPS), has been proposed, which combines uniform linear motion and stochastic reflection to perform sampling. BPS was reported to have the advantage of being easier to set simulation parameters than HMC. To accelerate the convergence to a posterior distribution, we introduced parallel tempering (PT) to BPS, and then proposed an algorithm when the inverse temperature exchange rate is set to infinity. We performed numerical simulations and demonstrated its effectiveness for multimodal distribution.

## 1 Introduction

One of the most important goals of learning is to predict unknown data from a finite number of known data. Therefore, it is desirable for a probability distribution used for predictions to have small deviations for all data including unknown ones (generalization error) rather than for a finite number of known data. Predictive distributions are usually obtained by adjusting the parameters included in a probability model based on known data. To obtain a predictive distribution with small generalization error, it is better to integrate the parameter of the probability model using the posterior distribution obtained by Bayesian inference as weights, rather than to substitute a single model parameter obtained by maximum likelihood estimation or maximum a posteriori (MAP) estimation into the probability model [1]. For this reason, Bayesian inference is employed in many fields, e.g. physics [2], biology [3], economics [4], and deep learning [5].

Although Bayesian inference is a useful estimation method, posterior distributions cannot be calculated analytically in most cases. Hence, we change a probability model to another one whose posterior distribution is easy to calculate (variational Bayesian inference) or approximate the posterior distribution by samples. Using sampling methods, we can approximate the posterior distribution with arbitrary accuracy if we take a sufficiently long computation time. Markov chain Monte Carlo (MCMC) [6] has been used for the sample approximation of discrete probability distributions, and Langevin Monte Carlo (LMC) [7] or Hamiltonian Monte Carlo (HMC) [8] has been used for the sample approximation of continuous probability distributions. In case of a probability distribution that has continuous and discrete variables, we usually use HMC after mapping the discrete variable to a continuous variable [9] or stochastically choosing the continuous variable by HMC or the discrete variable by MCMC [10] to update.

A method for sampling a continuous probability distribution has been devised using uniform linear motion and stochastic reflection and is called the bouncy particle sampler (BPS) [11, 12]. The BPS is a kind of non-reversible sampling using a piecewise-deterministic Markov process and is studied on theoretical aspects [13, 14], improvements [15, 16], and applications [17, 18]. By appropriately setting the transition probability between discrete states, the BPS can be applied to mixed continuous-discrete distributions [19]. BPS was reported to have the advantage that it is easier to adjust simulation parameters than HMC [12].

In sampling dynamics, situations often occur that when a particle moves from one high-probability region to another, it must pass through a low probability region. In this case, transitions between high-probability regions

<sup>\*</sup>ysaito366249@gunma-u.ac.jp, corresponding author

<sup>†</sup>koujin.takeda.kt@vc.ibaraki.ac.jp

rarely occur, and as a result, the distribution of positions of the particle slowly converges to the target distribution. Introducing temperature to reduce the variation in the probability distribution makes such transitions more likely to occur. Particles move in parallel in systems with different temperatures, and the positions of particles at different temperatures are exchanged at an appropriate event rate. This allows transitions between high-probability regions on the original target distribution without passing through low-probability regions, resulting in faster convergence. This method is called parallel tempering (PT) [20, 21] and is used in combination with various sampling algorithms, e.g. MCMC, LMC, and HMC. The higher the exchange rate in PT, the faster the convergence to the target distribution, and an algorithm has been proposed for LMC with PT that takes the infinite exchange limit [22]. The same situation occurs in the dynamics of BPS. In this paper, we first incorporate PT into BPS and propose an algorithm in infinite exchange limit. Then, we confirm the usefulness of BPS-PT with infinite exchange rate by numerical simulations.

This paper is organized as follows. Section 2 reviews the BPS for continuous probability distributions and for mixed continuous-discrete probability distributions. Section 3 introduces BPS incorporating PT and proposes BPS-PT with infinite exchange rate. Section 4 performs numerical simulations and confirms that BPS-PT with infinite exchange rate is more useful to a multimodal distribution than regular BPS. In Section 5, we summarize the paper.

## 2 Review of the bouncy particle sampler

There are many methods to sample from probability distributions where the normalization constant cannot be evaluated. MCMC [6] has been widely used for discrete probability distributions, and HMC [23] and its improved form No-U-Turn Sampler (NUTS) [24] have been widely used for continuous probability distributions. BPS [11, 12] is a method for obtaining samples from continuous probability distributions by a stochastically bouncing particle moving in a straight line with constant velocity. In this section, following Refs. [12, 19], we first explain BPS for continuous distributions and then explain BPS for mixed continuous-discrete distributions.

### 2.1 BPS for continuous distributions

Let  $p(x) \propto e^{-U(x)}$  be the target distribution, where  $x \in \mathbb{R}^n$  is a continuous variable. BPS is a method that combines elastic collisions with the potential surface  $U$  and uniform linear motion and obtains the target distribution as the long-term limit of the particle position distribution. The elastic collisions are generated by an inhomogeneous Poisson process whose event rate is given by

$$\lambda^b(x, v) = \alpha^b \max\{0, \langle v, \nabla U(x) \rangle\}, \quad (1)$$

where  $x \in \mathbb{R}^n$  and  $v \in \mathbb{R}^n$  are the position and velocity of the particle, respectively, and  $\alpha^b > 0$ . After an elastic collision, the velocity of the particle changes to

$$R(x)v = v - 2 \frac{\langle v, \nabla U(x) \rangle}{\|\nabla U(x)\|^2} \nabla U(x). \quad (2)$$

Using a sufficient regular function  $f: \mathbb{R}^n \times \mathbb{R}^n \rightarrow \mathbb{R}$ , the infinitesimal generator of BPS is written as

$$\mathcal{L}_{\text{BPS}}f(x, v) = \lambda^b(x, v)\{f(x, R(x)v) - f(x, v)\} + \lambda^{\text{ref}} \int \psi(v')\{f(x, v') - f(x, v)\}dv' + \langle v, \nabla_x f(x, v) \rangle, \quad (3)$$

$$\psi(v) = \frac{1}{(2\pi)^{d/2}} \exp\left[-\frac{1}{2}\|v\|^2\right], \quad (4)$$

where  $\lambda^{\text{ref}} > 0$ . The first term of Eq. (3) expresses a stochastic elastic collision of the particle. To satisfy the ergodic property, the velocity of the particle is stochastically refreshed by the standard normal distribution  $\psi$  in the second term of Eq. (3). The third term of Eq. (3) denotes the uniform linear motion. From the ergodic property and

$$\int \mathcal{L}_{\text{BPS}}f(x, v)p(x)\psi(v)dx dv = 0, \quad (5)$$

$p(x)\psi(v)$  is the stationary distribution of the infinitesimal generator. Therefore, using the dynamics generated by  $\mathcal{L}_{\text{BPS}}$ , we can obtain samples from the target distribution  $p$ . To simulate the inhomogeneous Poisson process

---

**Algorithm 1** BPS for a continuous probability distribution

---

```
1: Input  $\Delta t, N, \alpha^b, \lambda^{\text{ref}}$ 
2: Initialize  $x, v$ 
3:  $n \leftarrow 1, t \leftarrow 0$ 
4: while  $n \leq N$  do
5:    $\Delta t^{\text{ref}} \leftarrow -\ln r / \lambda^{\text{ref}}$  where  $r \sim \text{Uniform}(0, 1)$ 
6:   Determine  $\Delta t^b$  from a thinning algorithm
7:    $\Delta t^{\text{ev}} \leftarrow \min\{\Delta t^{\text{ref}}, \Delta t^b\}$ 
8:   if  $t + \Delta t^{\text{ev}} \geq n\Delta t$  then
9:     Sample  $(x + v(n\Delta t - t), v)$ 
10:     $n \leftarrow n + 1$ 
11:   end if
12:    $t \leftarrow t + \Delta t^{\text{ev}}$ 
13:    $x \leftarrow x + v\Delta t^{\text{ev}}$ 
14:   if  $\Delta t^{\text{ev}} = \Delta t^{\text{ref}}$  then
15:      $v \sim \mathcal{N}(0, 1)$ 
16:   else
17:      $v \leftarrow R(x)v$ 
18:   end if
19: end while
```

---

---

**Algorithm 2** Evaluation of an elastic collision time by thinning algorithm

---

```
1: Input  $\alpha^b, x, v$ 
2:  $\Delta t^b \leftarrow 0$ 
3: while true do
4:   Find  $\tilde{\lambda}^b$  which satisfies  $\tilde{\lambda}^b(x + vt, v) \geq \lambda^b(x + vt, v), \forall t \in [0, T]$  for some  $T$ 
5:   Find  $\Delta t$  which satisfies  $\ln r = -\int_0^{\Delta t} \tilde{\lambda}^b(x + vt, v)dt$  where  $r \sim \text{Uniform}(0, 1)$ 
6:   if  $\Delta t \leq T$  then
7:     if  $\lambda^b(x + v\Delta t, v) / \tilde{\lambda}^b(x + v\Delta t, v) \leq u$  where  $u \sim \text{Uniform}(0, 1)$  then
8:       return  $\Delta t^b + \Delta t$ 
9:     else
10:       $x \leftarrow x + v\Delta t, \Delta t^b \leftarrow \Delta t^b + \Delta t$ 
11:    end if
12:  else
13:     $x \leftarrow x + vT, \Delta t^b \leftarrow \Delta t^b + T$ 
14:  end if
15: end while
```

---

generated by Eq. (1), we employ the thinning algorithm [25], which requires an upper bound of the event rate  $\tilde{\lambda}^b$  in some time interval  $t \in [0, T]$ ,

$$\lambda^b(x + vt, v) \leq \tilde{\lambda}^b(x + vt, v), \quad (6)$$

whose event time can be analytically evaluated. For example, we can find a polynomial upper bound from the Taylor expansion of the directional derivative of  $\lambda^b$ . We show a pseudocode of BPS in Algs. 1, 2.

To approximate the target distribution with as few samples as possible, it is desirable that the samples are independently obtained from the target distribution. Thus, the performance of the algorithm is often evaluated by the effective sample size (ESS) [26] which corrects the number of samples for the intersample correlation. When comparing the ESS per simulation time, BPS is slightly inferior to HMC. However, BPS has the advantage that it does not require tuning the parameters used in the simulation ( $\alpha^b, \lambda^{\text{ref}}$ , sampling time) [12].

## 2.2 BPS for mixed continuous-discrete distributions

Let  $p(x, y) \propto e^{-U(x, y)}$  be the target distribution, where  $x \in \mathbb{R}^n$  and  $y \in S$  are continuous and discrete variables, respectively ( $S$  is a finite or countable set). Sampling dynamics for the mixed continuous-discrete distribution,

---

**Algorithm 3** BPS for a distribution of continuous and discrete variables

---

```
1: Input  $\Delta t, N, \alpha^b, \alpha^j, w, \lambda^{\text{ref}}$ 
2: Initialize  $x, y, v$ 
3:  $n \leftarrow 1, t \leftarrow 0$ 
4: while  $n \leq N$  do
5:    $\Delta t^{\text{ref}} \leftarrow -\ln r / \lambda^{\text{ref}}$  where  $r \sim \text{Uniform}(0, 1)$ 
6:   Determine  $\Delta t^{b,j}$  and  $(x', y', v')$  from thinning algorithm
7:    $\Delta t^{\text{ev}} \leftarrow \min\{\Delta t^{\text{ref}}, \Delta t^{b,j}\}$ 
8:   if  $t + \Delta t^{\text{ev}} \geq n\Delta t$  then
9:     Sample  $(x + v(n\Delta t - t), y, v)$ 
10:     $n \leftarrow n + 1$ 
11:   end if
12:    $t \leftarrow t + \Delta t^{\text{ev}}$ 
13:   if  $\Delta t^{\text{ev}} = \Delta t^{\text{ref}}$  then
14:      $x \leftarrow x + v\Delta t^{\text{ev}}$ 
15:      $v \sim \mathcal{N}(0, 1)$ 
16:   else
17:      $(x, y, v) \leftarrow (x', y', v')$ 
18:   end if
19: end while
```

---

including BPS [19], is constructed by inserting an update of the discrete variable into the dynamics of the continuous variable [10]. The discrete variable is updated by the Markov chain with transition probability  $w$  which satisfies the balance condition,

$$\sum_{y' \neq y} w(x, y' | x, y) p(x, y) = \sum_{y \neq y'} w(x, y | x, y') p(x, y'). \quad (7)$$

Using a sufficient regular function  $f: \mathbb{R}^n \times S \times \mathbb{R}^n \rightarrow \mathbb{R}$ , the infinitesimal generator of BPS is given by

$$\begin{aligned} \mathcal{L}'_{\text{BPS}} f(x, y, v) = & \lambda^b(x, y, v) \{f(x, y, R(x, y)v) - f(x, y, v)\} + \sum_{y' \neq y} \lambda^j(x, y, y') \{f(x, y', v) - f(x, y, v)\} \\ & + \lambda^{\text{ref}} \int \psi(v') \{f(x, y, v') - f(x, y, v)\} dv' + \langle v, \nabla_x f(x, y, v) \rangle, \end{aligned} \quad (8)$$

$$\lambda^j(x, y, y') = \alpha^j w(x, y' | x, y), \quad (9)$$

where  $\alpha^j > 0$ . Since transition events are also an inhomogeneous Poisson process, we employ a thinning algorithm that uses an upper bound of the total event rate, that is, the sum of the reflections and the transitions. If we use the Metropolis–Hastings (MH) method and the detailed balance condition to make the transition probability, we can always choose an upper bound  $w(x, y' | x, y) \leq 1$ . Thus, it is easy to find an upper bound if we do not take into account the rejection rate of the thinning algorithm. We show a pseudocode in Algs. 3, 4.

### 3 BPS-PT with infinite exchange rate

In sampling dynamics, we often find that when a particle moves from one high-probability region to another it must pass through a low-probability region. In this case, the distribution of the position of the particle slowly converges to the target distribution. PT [20, 21] has been used to solve this problem. That is, introduce inverse temperatures,  $1 = \beta_1 > \dots > \beta_L > 0$ , into the probability distribution as  $p^{\beta_i}(x, y) \propto e^{-\beta_i U(x, y)}$ , move the particles in each distribution in parallel, and then exchange the positions of the particles. As the inverse temperature decreases, the variation of the probability distribution decreases, and the particle moves more frequently a wider region. By exchanging the positions of the particles between different inverse temperatures, the particle at  $\beta_1$  moves from one high-probability region to another without passing through low-probability regions, which accelerates the convergence to the target distribution. In LMC, it was shown that the convergence to the target distribution speeds up as the exchange rate increases [22], and LMC with infinite exchange PT was proposed in Ref. [22]. In this section, we introduce PT with finite and infinite exchange rate to BPS.

---

**Algorithm 4** Evaluation of an elastic collision time and transition time by thinning algorithm

---

```

1: Input  $\alpha^b, \alpha^j, w, x, y, v$ 
2:  $\lambda^{b,j}(\cdot, y, v) = \lambda^b(\cdot, v) + \sum_{y' \neq y} \lambda^j(\cdot, y, y')$ 
3:  $\Delta t^{b,j} \leftarrow 0$ 
4: while true do
5:   Find  $\tilde{\lambda}^{b,j}$  which satisfies  $\tilde{\lambda}^{b,j}(x + vt, y, v) \geq \lambda^{b,j}(x + vt, y, v), \forall t \in [0, T]$  for some  $T$ 
6:   Find  $\Delta t$  which satisfies  $\ln r = - \int_0^{\Delta t} \tilde{\lambda}^{b,j}(x + vt, y, v) dt$  where  $r \sim \text{Uniform}(0, 1)$ 
7:   if  $\Delta t \leq T$  then
8:      $\Delta t^{b,j} \leftarrow \Delta t^{b,j} + \Delta t$ 
9:     if  $\lambda^{b,j}(x + v\Delta t, y, v) / \tilde{\lambda}^{b,j}(x + v\Delta t, y, v) \leq u$  where  $u \sim \text{Uniform}(0, 1)$  then
10:      if  $\lambda^b(x + v\Delta t, y, v) / \lambda^{b,j}(x + v\Delta t, y, v) \leq u'$  where  $u' \sim \text{Uniform}(0, 1)$  then
11:         $x' \leftarrow x + v\Delta t, y' \leftarrow y$ 
12:         $v' \leftarrow R(x, y)v$ 
13:      else
14:         $y' \sim \text{Cat}(w(x + v\Delta t, y, \cdot))$ 
15:         $x' \leftarrow x + v\Delta t, v' \leftarrow v$ 
16:      end if
17:      return  $\Delta t^{b,j}$  and  $(x', y', v')$ 
18:    else
19:       $x \leftarrow x + v\Delta t$ 
20:    end if
21:  else
22:     $x \leftarrow x + vT, \Delta t^{b,j} \leftarrow \Delta t^{b,j} + T$ 
23:  end if
24: end while

```

---

### 3.1 BPS with PT

In most cases, PT exchanges particles between adjacent inverse temperatures using a homogeneous Poisson process. Since the particle positions change discontinuously before and after an exchange, a piecewise continuous trajectory cannot be obtained in the limit of infinite exchange rate. Instead of fixing the inverse temperatures and exchanging the particle positions, the authors of Ref. [22] fix the particle positions and exchange the inverse temperatures. Furthermore, they use the permutation group  $S_L$  to exchange inverse temperatures not only between particles with adjacent subscripts but also for all particles.

We introduce this kind of PT to BPS. The event rate that a particle set  $\{(x_i, y_i, v_i)\}_{i=1}^L$  changes the inverse temperature distribution from  $(\beta_{\sigma(1)}, \dots, \beta_{\sigma(L)})$  to  $(\beta_{\sigma'(1)}, \dots, \beta_{\sigma'(L)})$  is given by

$$g_{\sigma\sigma'}(x, y) = \min \left\{ 1, \frac{\prod_{i=1}^L p(x_i, y_i)^{\beta_{\sigma'(i)}}}{\prod_{i=1}^L p(x_i, y_i)^{\beta_{\sigma(i)}}} \right\}, \quad (10)$$

where  $\alpha^s > 0$ . Using a sufficiently regular function  $f: \mathbb{R}^n \times S \times \mathbb{R}^n \times S_L \rightarrow \mathbb{R}$ , the infinitesimal generator of BPS-PT with a finite exchange rate is written as

$$\begin{aligned}
\mathcal{L}_{\text{BPSPT}} f(x, y, v, z) = & \sum_{\sigma \in S_L} 1_{z=\sigma} \left[ \sum_{i=1}^L \left\{ \lambda_{\sigma(i)}^b(x_i, y_i, v_i) \{f(x, y, R_i(x_i, y_i)v, z) - f(x, y, v, z)\} \right. \right. \\
& + \sum_{y'_i \neq y_i} \lambda_{\sigma(i)}^j(x_i, y_i, y'_i) \{f(x, R'_i(y'_i)y, v, z) - f(x, y, v, z)\} \\
& + \lambda^{\text{ref}} \int \psi(v'_i) \{f(x, y, R'_i(v'_i)v, z) - f(x, y, v, z)\} dv'_i \Big\} \\
& + \alpha^s \sum_{\sigma' \neq \sigma} g_{z, \sigma'}(x, y) \{f(x, y, v, \sigma') - f(x, y, v, z)\} + \langle v, \nabla_x f(x, y, v, z) \rangle \Big], \quad (11)
\end{aligned}$$

where

$$R_i(x_i, y_i)v = (v_1, \dots, v_{i-1}, R(x_i, y_i)v_i, v_{i+1}, \dots, v_L), \quad (12)$$

$$R'_i(y'_i)y = (y_1, \dots, y_{i-1}, y'_i, y_{i+1}, \dots, y_L), \quad (13)$$

$$R'_i(v'_i)v = (v_1, \dots, v_{i-1}, v'_i, v_{i+1}, \dots, v_L). \quad (14)$$

Note that from Eq. (2), the velocity after an elastic collision is not affected by the inverse temperature. The reflection and transition rates are given by

$$\lambda_{\sigma(i)}^b(x_i, y_i, v_i) = \alpha^b \max\{0, \langle v, \beta_{\sigma(i)} \nabla_x U(x) \rangle\} = \beta_{\sigma(i)} \lambda^b(x_i, y_i, v_i), \quad (15)$$

$$\lambda_{\sigma(i)}^j(x_i, y_i, y'_i) = \alpha^j w_{\sigma(i)}(x_i, y'_i | x_i, y_i), \quad (16)$$

$$\sum_{y'_i \neq y_i} w_{\sigma(i)}(x_i, y'_i | x_i, y_i) p(x_i, y_i)^{\beta_{\sigma(i)}} = \sum_{y_i \neq y'_i} w_{\sigma(i)}(x_i, y_i | x_i, y'_i) p(x_i, y'_i)^{\beta_{\sigma(i)}}. \quad (17)$$

BPS-PT with a finite exchange rate can be simulated by the inhomogeneous Poisson process whose event rate is given by the sum of the reflections, transitions, and exchange of the inverse temperatures;

$$\sum_{i=1}^L \left[ \lambda_{z(i)}^b(x_i + v_i t, y_i, v_i) + \sum_{y'_i \neq y_i} \lambda_{z(i)}^j(x_i + v_i t, y_i, y'_i) \right] + \alpha^s \sum_{\sigma' \neq z} g_{z, \sigma'}(x + vt, y). \quad (18)$$

Due to the symmetry of the particles, the stationary distribution is

$$P_{\text{st}}(x, y, v) \propto \frac{1}{L!} \sum_{\sigma \in S_L} \prod_{i=1}^L p(x_i, y_i)^{\beta_{\sigma(i)}} \psi(v_i). \quad (19)$$

Similarly to Ref. [22], to obtain the same sampling as with PT that exchanges the particle positions, we rearrange the particle positions using the temperature distribution at each time,  $z(t)$ , as

$$\eta_{\alpha^s}(T) = \frac{1}{T} \int_0^T \sum_{\sigma \in S_L} 1_{z(t)=\sigma} \delta_{(\sigma^{-1}(x(t)), \sigma^{-1}(y(t)), v(t))} dt, \quad (20)$$

$$\sigma^{-1}(x(t)) = (x_{\sigma^{-1}(1)}(t), \dots, x_{\sigma^{-1}(L)}(t)), \quad (21)$$

which converges to the target distribution  $\prod_{i=1}^L p(x_i, y_i)^{\beta_i} \psi(v_i)$  in  $T \rightarrow \infty$ . In this way, we can obtain samples from the target distribution.

### 3.2 Infinite swapping rate limit of BPS-PT

As already mentioned, the higher the exchange rate  $\alpha^s$  of PT, the faster the convergence to the target distribution. Therefore, it is desirable to take it to the limit of infinity. Referring to Ref. [22], the infinitesimal generator of BPS-PT with infinite exchange rate is written as

$$\begin{aligned} \mathcal{L}_{\text{BPSPT}}^\infty f(x, y, v) = & \sum_{i=1}^L \left[ \lambda_i^{\infty, b}(x_i, y_i, v_i) \{f(x, y, R_i(x_i, y_i)v) - f(x, y, v)\} \right. \\ & + \sum_{y'_i \neq y_i} \lambda_i^{\infty, j}(x_i, y_i, y'_i) \{f(x, R'_i(y'_i)y, v) - f(x, y, v)\} \\ & \left. + \lambda^{\text{ref}} \int \psi(v'_i) \{f(x, y, R'_i(v'_i)v) - f(x, y, v)\} dv'_i \right] + \langle v, \nabla_x f(x, y, v) \rangle, \end{aligned} \quad (22)$$

where the reflection and transition rates are given by

$$\lambda_i^{\infty, b}(x_i, y_i, v_i) = \sum_{\sigma \in S_L} \beta_{\sigma(i)} \omega_\sigma(x, y) \lambda^b(x_i, y_i, v_i), \quad (23)$$

$$\lambda_i^{\infty, j}(x_i, y_i, y'_i) = \sum_{\sigma \in S_L} \omega_\sigma(x, y) w_{\sigma(i)}(x_i, y'_i | x_i, y_i), \quad (24)$$

$$\omega_\sigma(x, y) = \frac{\prod_{i=1}^L p(x_i, y_i)^{\beta_{\sigma(i)}}}{\sum_{\sigma' \in S_L} \prod_{i=1}^L p(x_i, y_i)^{\beta_{\sigma'(i)}}}. \quad (25)$$

Intuitively, due to an infinitely large exchange rate, the particles exchange infinitely many times and the inverse temperature distribution instantaneously reaches the stationary distribution fixed at  $x, y$  at that time,

$$P_{x,y}(\sigma) \propto \omega_\sigma(x, y). \quad (26)$$

Therefore, by replacing  $1_{z=\sigma}$  in Eq. (11) with the stationary distribution  $\omega_\sigma(x, y)$ , we obtain the generator of BPT-PT with infinite exchange rate.

As can be seen from Eq. (24), we have to evaluate the transition probability at all inverse temperatures and for each particle, which increases the computational cost compared to BPS-PT with a finite exchange rate. From Eq. (23), the reflection rate only requires calculating  $\lambda^b$ . Thus, if the target distribution is a continuous distribution, the computational cost is approximately the same as that of BPS-PT with a finite exchange rate. The stationary distribution is the same as that of the BPS-PT with a finite exchange rate and is given by Eq. (19). Similarly to Eq. (20), the distribution of the position of the particles after rearranging,

$$\eta_\infty(T) = \frac{1}{T} \int_0^T \sum_{\sigma \in S_L} \omega_\sigma(x(t), y(t)) \delta_{(\sigma^{-1}(x(t)), \sigma^{-1}(y(t)), v(t))} dt, \quad (27)$$

converges to the target distribution in  $T \rightarrow \infty$ .

As the number of inverse temperatures  $L$  increases, the number of elements in the permutation group increases rapidly, making it impossible to take the sum over the elements in the permutation group. Therefore, as in Ref. [22], we use a lightweight version that uses generating subgroups of  $S_L$ . For example, we can find two generating subgroups,  $G$  and  $G'$ , as follows. First, we divide  $\{1, \dots, L\}$  into two different partitions that satisfy

$$\{1, \dots, L\} = \bigcup_{i=1}^N A_i = \bigcup_{i=1}^N B_i, \quad A_1 \subsetneq B_1, \quad B_{i-1} \cap A_i \neq \emptyset, \quad A_i \cap B_i \neq \emptyset, \quad B_N \subsetneq A_N \quad (i = 2, \dots, N). \quad (28)$$

Then consider the products of the permutation groups within the subsets,  $G = S_{|A_1|} \times \dots \times S_{|A_N|}$  and  $G' = S_{|B_1|} \times \dots \times S_{|B_N|}$ . Since any element in  $S_L$  can be expressed as a finite product of elements in  $G$  and  $G'$ , they are generating subgroups of  $S_L$ . Instead of  $S_L$ , we alternately use  $G$  and  $G'$  to exchange the inverse temperatures at each interval  $t_\beta$ . The reflection and transition rate for  $G$  are given as follows. Suppose that  $i \in A_l$  when we divide  $\{1, \dots, L\}$  into  $A_1, \dots, A_N$ , and an upper bound of  $\lambda^b$  in time interval  $[0, T]$  is  $\tilde{\lambda}^b$ . Then, the reflection and transition rate of the  $i$ -th particle and their upper bound are given by

$$\begin{aligned} \lambda_i^{\infty, b}(x_i + v_i t, y_i, v_i) &= \sum_{\sigma \in S_{|A_l|}} \beta_{\sigma(i)} \omega_{l, \sigma}(x, y) \lambda^b(x_i + v_i t, y_i, v_i) \\ &\leq \sum_{\sigma \in S_{|A_l|}} \beta_{\sigma(i)} \omega_{l, \sigma}(x, y) \tilde{\lambda}^b(x_i + v_i t, y_i, v_i) \leq (\max_{j \in A_l} \beta_j) \tilde{\lambda}^b(x_i + v_i t, y_i, v_i), \end{aligned} \quad (29)$$

$$\lambda_i^{\infty, j}(x_i, y_i, y'_i) = \alpha^j \sum_{\sigma \in S_{|A_l|}} \omega_{l, \sigma}(x, y) w_{\sigma(i)}(x_i, y'_i | x_i, y_i) \leq \alpha^j \sum_{\sigma \in S_{|A_l|}} \omega_{l, \sigma}(x, y) = \alpha^j, \quad (30)$$

$$\omega_{l, \sigma}(x, y) = \frac{\prod_{j \in A_l} p(x_j, y_j)^{\beta_{\sigma(j)}}}{\sum_{\sigma' \in A_l} \prod_{j \in A_l} p(x_j, y_j)^{\beta_{\sigma'(j)}}}, \quad (31)$$

and an upper bound of the total event rate in  $A_l$ ,  $\tilde{\Lambda}_l$ , can be expressed by

$$\tilde{\Lambda}_l(x + vt, y, v) = (\max_{i \in A_l} \beta_i) \sum_{i \in A_l} \tilde{\lambda}^b(x_i + v_i t, y_i, v_i) + |A_l| \alpha^j. \quad (32)$$

After time  $t_\beta$  has passed, we determine the inverse temperature ordering of the particles using  $\prod_{l=1}^N \omega_{l, \sigma_l}(x, y)$  and switch to the other subgroup  $G'$ . The shorter the subgroup switching time  $t_\beta$ , the closer the method will be to use  $S_L$ , although the computational cost increases. Thus, we should set  $t_\beta$  appropriately short, depending on the problem. After switching the subgroups several times, we evaluate  $\prod_{l=1}^N \omega_{l, \sigma_l}(x, y)$  to determine the inverse temperature ordering and can obtain a sample from each  $p^{\beta_i}$  ( $i = 1, \dots, L$ ). By sampling and switching the subgroups at the same time, we can reduce the number of calculations of  $\prod_{l=1}^N \omega_{l, \sigma_l}(x, y)$  by one. In this paper, we set the sampling time as  $n_s t_\beta$  for an integer  $n_s$ . We show a pseudocode in Algs. 5, 6, 7.

---

**Algorithm 5** BPS-PT with infinite exchange rate

---

```
1: Input  $n_s, t_\beta, N, \alpha^b, \alpha^j, w, G, G', \lambda^{\text{ref}}, \{\beta_1, \dots, \beta_L\}$ 
2: Initialize  $\{(x_i, y_i, v_i)\}_{i=1}^L$ 
3:  $n \leftarrow 1, m \leftarrow 1, t \leftarrow 0, H \leftarrow G$ 
4: while  $n \leq N$  do
5:   if  $H = G$  then
6:     for  $A \in \{A_1, \dots, A_N\}$  do
7:       Generate  $\{(x_i, y_i, v_i)\}_{i \in A}$  after  $t_\beta$ 
8:     end for
9:      $H \leftarrow G'$ 
10:  else
11:    for  $B \in \{B_1, \dots, B_N\}$  do
12:      Generate  $\{(x_i, y_i, v_i)\}_{i \in B}$  after  $t_\beta$ 
13:    end for
14:     $H \leftarrow G$ 
15:  end if
16:   $m \leftarrow m + 1$ 
17:  if  $m = n_s$  then
18:    Sample  $\{(x_i, y_i, v_i)\}_{i=1}^L$ 
19:     $n \leftarrow n + 1, m \leftarrow 1$ 
20:  end if
21: end while
```

---

## 4 Numerical simulation

We applied and compared regular BPS and BPS-PT with infinite exchange rate to the Gaussian mixture model used in Ref. [9] and the mixed continuous-discrete distribution [27] used in Refs. [27, 10]. In the following, we simply write BPS-PT with infinite exchange rate as BPS-PT. We employed the two-sample Kolmogorov-Smirnov (KS) test and the ESS as evaluation metrics for continuous variable, and Kullback-Leibler divergence (KLD) or the mean squared error (MSE) for discrete variable. In the two-sample KS test, we used the marginal empirical distribution with respect to each component of the continuous variable. We used the minimum of the ESS for each component of the continuous variable as the ESS. All experiments were run on a machine with Intel(R) Core(TM) i7-14700 CPU, and 32 GB RAM. For comparison, we used Metropolis augmented HMC (MAHMC) [10] in <https://github.com/StannisZhou/mahmc>.

---

**Algorithm 6** Time translation of BPS-PT using a subgroup  $G$ 

---

```
1: Input  $t_\beta, \alpha^b, \alpha^j, w, A_l, \lambda^{\text{ref}}, \{\beta_i\}_{i \in A_l}, \{(x_i, y_i, v_i)\}_{i \in A_l}$ 
2:  $t \leftarrow 0$ 
3: while  $t < t_\beta$  do
4:    $\Delta T^{\text{ref}} \leftarrow \{-\ln r_i / \lambda^{\text{ref}} \mid i \in A_l\}$  where  $r_i \sim \text{Uniform}(0, 1)$ 
5:    $\Delta t^{\text{ev}} \leftarrow \min \Delta T^{\text{ref}}, i^{\text{ev}} \leftarrow \arg \min \Delta T^{\text{ref}}$ 
6:   Determine  $\Delta t^{\text{ev}}$  and  $\{(x'_i, y'_i, v'_i)\}_{i \in A_l}$  from thinning algorithm
7:   if  $t + \Delta t^{\text{ev}} \geq t_\beta$  then
8:      $\{x_i\}_{i \in A_l} \leftarrow \{x_i + v_i(t_\beta - t)\}_{i \in A_l}$ 
9:      $\sigma \sim \omega_{l, \cdot}(x, y)$ 
10:    return  $\{(x_{\sigma^{-1}(i)}, y_{\sigma^{-1}(i)}, v_i)\}_{i \in A_l}$ 
11:  else
12:     $\{(x_i, y_i, v_i)\}_{i \in A_l} \leftarrow \{(x'_i, y'_i, v'_i)\}_{i \in A_l}, t \leftarrow t + \Delta t^{\text{ev}}$ 
13:  end if
14: end while
```

---



---

**Algorithm 7** Update of variables by thinning algorithm in an inverse temperature subset

---

```
1: Input  $\alpha^b, \alpha^j, w, \{(x_i, y_i, v_i)\}_{i \in A_l}, A_l, \Delta t^{\text{ev}}, i^{\text{ev}}$ 
2:  $\Delta t^{\text{b,j}} \leftarrow 0$ 
3:  $\lambda^{\text{b,j}}(\cdot, \{y_i\}_{i \in A_l}, \{v_i\}_{i \in A_l}) = \sum_{i \in A_l} [\lambda_i^{\infty, \text{b}}(\cdot, y_i, v_i) + \sum_{y'_i \neq y_i} \lambda_i^{\infty, \text{j}}(\cdot, y_i, y'_i)]$ 
4: while  $\Delta t^{\text{b,j}} < t^{\text{ev}}$  do
5:   Find  $\tilde{\lambda}^{\text{b,j}}$  which satisfies  $\tilde{\lambda}^{\text{b,j}}(x + vt, y, v) \geq \lambda^{\text{b,j}}(x + vt, y, v), \forall t \in [0, T]$  for some  $T \leq t^{\text{ev}} - \Delta t^{\text{b,j}}$ 
6:   Find  $\Delta t$  which satisfies  $\ln r = - \int_0^{\Delta t} \tilde{\lambda}^{\text{b,j}}(x + vt, y, v) dt$  where  $r \sim \text{Uniform}(0, 1)$ 
7:   if  $\Delta t \leq T$  then
8:      $\Delta t^{\text{b,j}} \leftarrow \Delta t^{\text{b,j}} + \Delta t$ 
9:     if  $\lambda^{\text{b,j}}(x + v\Delta t, y, v) / \tilde{\lambda}^{\text{b,j}}(x + v\Delta t, y, v) \leq u$  where  $u \sim \text{Uniform}(0, 1)$  then
10:        $x' \leftarrow x + v\Delta t, y' \leftarrow y, v' \leftarrow v$ 
11:        $q \leftarrow (\lambda_i^{\infty, \text{b}}(x_i + v_i\Delta t, y_i, v_i), (\lambda_i^{\infty, \text{j}}(x_i + v_i\Delta t, y_i, y'_i))_{y'_i \neq y_i})_{i \in A} / \lambda^{\text{b,j}}(x + v\Delta t, y, v)$ 
12:       Choose event and particle index  $\tilde{i}^{\text{ev}}$  from  $\text{Cat}(q)$ 
13:        $\Delta t^{\text{ev}} \leftarrow \Delta t^{\text{b,j}} + \Delta t, i^{\text{ev}} \leftarrow \tilde{i}^{\text{ev}}$ 
14:       if event is bounce then
15:          $v'_{i^{\text{ev}}} \leftarrow R(x_{i^{\text{ev}}}, y_{i^{\text{ev}}})v_{i^{\text{ev}}}$ 
16:       else
17:          $y'_{i^{\text{ev}}} \sim \text{Cat}(w(x_{i^{\text{ev}}} + v_{i^{\text{ev}}}\Delta t, y_{i^{\text{ev}}}, \cdot))$ 
18:       end if
19:       return  $\Delta t^{\text{ev}}$  and  $(x', y', v')$ 
20:     else
21:        $x \leftarrow x + v\Delta t, \Delta t^{\text{b,j}} \leftarrow \Delta t^{\text{b,j}} + \Delta t$ 
22:     end if
23:   else
24:      $x \leftarrow x + vT, \Delta t^{\text{b,j}} \leftarrow \Delta t^{\text{b,j}} + T$ 
25:   end if
26: end while
27:  $x' \leftarrow x + v\Delta t^{\text{ev}}, y' \leftarrow y, v' \leftarrow v$ 
28:  $v'_{i^{\text{ev}}} \sim \mathcal{N}(0, 1)$ 
29: return  $\Delta t^{\text{ev}}, (x', y', v')$ 
```

---

## 4.1 Gaussian mixture model

The target distribution was the 24-dimensional 4-component Gaussian mixture model used in Ref. [9]. The cluster probabilities were 0.15, 0.3, 0.3, 0.25, the cluster centers were given by all permutations of  $-2, 0, 2, 4$ , and all covariance matrices were  $3I$ . The inverse temperatures were  $\beta_i = 1.0 - 0.1(i - 1)$  ( $i = 1, \dots, 10$ ), and the partitions were  $\{\{1, \dots, 4\}, \{5, \dots, 8\}, \{9, 10\}\}$  and  $\{\{1, 2\}, \{3, \dots, 6\}, \{7, \dots, 10\}\}$ . The subgroup switching time was set to  $t_\beta = 0.1$ , and the sampling time was set to  $t_{\text{samp}} = 10t_\beta$ . The reflection, transition and refresh parameters were  $\alpha^b = 1, \alpha^j = 4, \lambda^{\text{ref}} = 1$ , and the cluster transition was performed by MCMC which did not satisfy the detailed balance condition [28]. (We did not tune the hyperparameters.) The number of samples was  $10^5$  for each 10 independent Markov chain. The computation time was  $(5.1 \pm 0.2) \times 10$  seconds for BPS and  $(3.2 \pm 0.1) \times 10^3$  seconds for BPS-PT. (The means and standard deviations were estimated from 10 trials.) Since BPS-PT evaluates the event rate for all of the permutations in the subset, the computation time of BPS-PT was approximately  $4! + 4! + 2 = 50$  times longer than BPS, which is a reason for the difference in computation time.

Next, we compared the samples from the BPS and BPS-PT with the target distribution. Tab. 1 shows the cluster probability estimates, that is, the number of samples with each cluster index divided by the number of samples, by BPS and BPS-PT. Since the covariances were too small to cover the distance between the cluster centers, the transition probabilities between the clusters were small. As a result, the number of transitions between clusters was insufficient in the computation time, which led the BPS to fail to estimate the cluster probabilities. The KLDs from the target discrete distribution to the sampling distribution were 0.1951 for BPS and 0.0011 for BPS-PT, and we find that PT significantly improved the estimates. Using samples obtained from the target distribution, the two-sample KS test value was calculated for each component of the continuous variable for each Markov chain, and we took an average with respect to the Markov chains. Fig. 1 shows the change in the maximum KS value with respect to the components of the continuous variable as a function of the number of samples. Due to an insufficient number of transitions between the clusters, the KS value for the BPS did not decrease in the sample size. In

contrast, the KS value for the BPS-PT decreases, and we find that the samples from the BPS-PT are much closer to the target distribution than those from the BPS. The ESS per sample was  $4 \times 10^{-4}$  in BPS and  $3.8 \times 10^{-3}$  in BPS-PT. The small ESS in BPS-PT can be explained as follows. Since ESS is evaluated by the autocorrelation of each component of the continuous variable, it depends on the reflection rate and the refresh rate. To compensate for a low reflection rate at low  $\beta$ , we set a refresh rate equal to the inverse of the sampling time, which reduced the inter-sample correlation. This prevented particle exchange from introducing inter-sample correlation in  $\beta = 1$ . We summarize the comparison in Tab. 2.

Finally, we compared BPS-PT with MAHMC. We tuned the hyperparameters by the grid search. In MAHMC, the KLD from the target discrete distribution to the sample distribution was 0.1341, the maximum value of the KS test value at  $10^5$  samples was 0.3791, and the ESS per sample was  $1.9 \times 10^{-6}$  ( $9 \times 10^5$  samples for each 16 independent Markov chain). Although the hyperparameters may not have been optimized, the performance was generally comparable to BPS. It took  $(7 \pm 2) \times 10^{-4}$  seconds to obtain the samples, which was much shorter than the computation time of the BPS. (The means and standard deviations were estimated from 10 trials.) However, taking into account the time for tuning the hyperparameters, the computation time of BPS and BPS-PT was not longer than that of MAHMC.

Table 1: Comparison of cluster probability estimates using BPS and BPS-PT samples. For BPS-PT, we only shows the cluster probability estimates for  $\beta = 1$ . We can find that the PT improves the estimation accuracy.

ground truth	0.15	0.3	0.3	0.25
BPS	0.100	0.500	0.100	0.300
BPS-PT	0.122	0.323	0.308	0.248

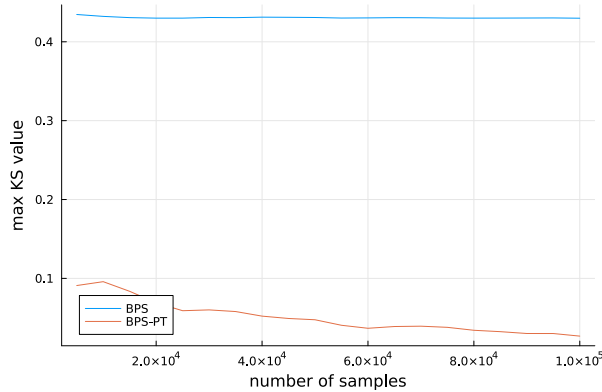


Figure 1: We show the maximum KS test values with respect to the components of the continuous variable as a function of the number of samples. Since the BPS failed to estimate the cluster probabilities, KS value for the BPS does not decrease as the number of samples increases. In contrast, KS value for the BPS-PT decreases with the number of samples.

Table 2: Comparison of computation time, maximum KS value, KLD, and ESS per sample is shown. BPS-PT was superior to BPS except for the computation time.

	computation time [sec]	max KS val	KLD	ESS per sample
BPS	$(5.1 \pm 0.2) \times 10$	$0.4 \pm 0.1$	0.1951	$4 \times 10^{-4}$
BPS-PT	$(3.2 \pm 0.1) \times 10^3$	$0.03 \pm 0.01$	0.0011	$3.8 \times 10^{-3}$

## 4.2 a mixed continuous-discrete distribution

We used the model proposed in Ref. [27],

$$x_1 \sim \mathcal{N}(x_1 | 0, 1), \quad x_2 | x_1 \sim \mathcal{N}(x_2 | x_1, 0.04), \quad y_i | x_1 \sim \text{Bernoulli}\left(\frac{1}{1 + e^{x_1}}\right) \quad (i = 1, \dots, 20). \quad (33)$$

As an upper bound of the reflection rate, we used the following linear function with respect to  $t$ ,

$$\begin{aligned}\lambda^b(x, y, v) &= x_1 v_1 + \frac{(x_2 - x_1)(v_2 - v_1)}{0.04^2} - v_1 \sum_{i=1}^N (1 - y_i) + \left[ \frac{(v_2 - v_1)^2}{0.04^2} + v_1^2 \right] t + v_1 \sum_{i=1}^N \frac{e^{x_1 + v_1 t}}{1 + e^{x_1 + v_1 t}} \\ &\leq x_1 v_1 + \frac{(x_2 - x_1)(v_2 - v_1)}{0.04^2} - v_1 \sum_{i=1}^N (1 - y_i) + \left[ \frac{(v_2 - v_1)^2}{0.04^2} + v_1^2 \right] t + \theta(v_1) v_1 N.\end{aligned}\quad (34)$$

The inverse temperatures used were  $\beta_i = 1.0 - 0.2(i - 1)$  ( $i = 1, \dots, 5$ ), and the partitions were  $\{\{1, 2, 3\}, \{4, 5\}\}$  and  $\{\{1, 2\}, \{3, 4, 5\}\}$ . The subgroup switching time was set to  $t_\beta = 0.1$ , and the sampling time was set to  $t_{\text{samp}} = 10t_\beta$ . The reflection, transition, and refresh parameters were  $\alpha^b = 1, \alpha^j = 20, \lambda^{\text{ref}} = 0.1$ . (We did not tune the hyperparameters.) We allowed transitions of the discrete variable that change one of its components. The transition probability was determined by the MH method using a uniform proposal distribution. The number of samples was  $3 \times 10^4$  for 10 independent Markov chains. The computation time is  $(6.0 \pm 0.3) \times 10$  seconds for BPS and  $(8.4 \pm 0.4) \times 10^2$  seconds for BPS-PT. (The means and standard deviations were estimated from 10 trials.) Although BPS-PT requires  $3! + 2! = 8$  combinations for each event rate, the computation time for BPS-PT increased more than 8 times compared to that for BPS. This was because the upper bound of the event rate,  $\tilde{\Lambda}_l$ , in Eq. (32) increased due to multiple  $\beta$ s, increasing the number of calculations of the event rate. (This effect was considered significant in this model because the reflection rate is high due to the small variance of  $x_2$ .)

Next, we compare the samples from the BPS and BPS-PT with the target distribution. The ground truth of the target discrete distribution is  $p(Y_i = 1) = 1/2$  for all  $i$ , and the MSEs between the ground truth and the sample distribution are  $1.4721 \times 10^{-6}$  in BPS and  $7.9956 \times 10^{-7}$  in BPS-PT. Using samples obtained from the target distribution, we calculated the KS test value for each component of the continuous variables. In Fig. 2, we find that both methods decreased the KS test value and BPS-PT is slightly superior to BPS. The ESS for BPS was 0.077 and that for BPS-PT was 0.198, showing that BPS-PT had a lower inter-sample correlation. Consequently, since this model is rather simple, the benefits of the PT were small and were not worth the increase in computation time. We summarize the comparison in Tab. 3.

Finally, we compared BPS-PT with MAHMC. We used the hyperparameters already tuned in <https://github.com/StannisZhou/mahmc/blob/main/mdc.ipynb>. In MAHMC, the MSE between the target discrete distribution and the sample distribution was  $7.0744 \times 10^{-8}$ , the maximum value of the KS test value at  $3 \times 10^4$  samples was 0.005, and the ESS per sample was 1.78236 ( $3 \times 10^4$  samples for each 10 independent Markov chain). Since the hyperparameters were optimized in Ref. [10], the performance was superior to BPS and BPS-PT in this model. It took  $(9 \pm 3) \times 10^{-4}$  seconds to obtain the samples, which was much shorter than the computation time of the BPS. (The means and standard deviations were estimated from 10 trials.) However, if we need to tune the hyperparameters, BPS is not considered to be a bad choice.

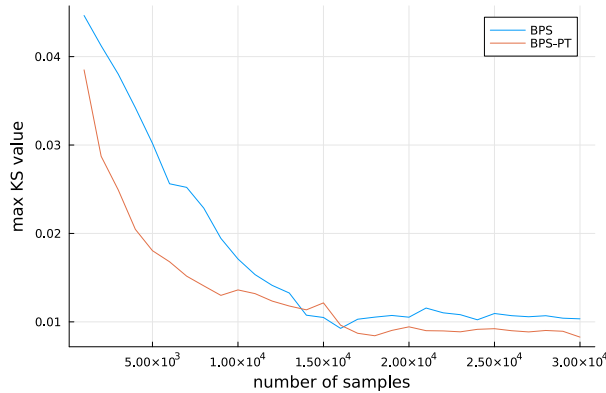


Figure 2: We show the maximum KS test values with respect to the components of the continuous variable as a function of the number of samples. KS value decreases in both methods, and KS value in BPS-PT is slightly smaller than that in BPS.

Table 3: Comparison of computation time, maximum KS value, MSE, and ESS per sample is shown. Although BPS-PT was superior to BPS, the increase in computation time was not worth it.

	computation time [sec]	max KS val	MSE	ESS per sample
BPS	$(6.0 \pm 0.3) \times 10$	$(1.0 \pm 0.5) \times 10^{-2}$	$1.4721 \times 10^{-6}$	0.077
BPS-PT	$(8.4 \pm 0.4) \times 10^2$	$(8 \pm 3) \times 10^{-3}$	$7.9956 \times 10^{-7}$	0.198

## 5 Summary

Bayesian inference is superior to point estimations in terms of the generalization error [1]. However, in most cases, the posterior distribution cannot be calculated analytically, and variational Bayesian inference or sample approximation is employed. Although HMC [8] is widely used for sample approximation, BPS, a sample method using uniform linear motion and stochastic reflections, has been reported to have the advantage of making it easier to adjust the simulation parameters [12]. A sample distribution can get arbitrarily close to the target distribution if it takes enough computation time. However, depending on the combination of the target distribution and sampling dynamics, convergence can be slow. Thus, PT has been proposed to accelerate convergence by exchanging particles at several inverse temperatures [20, 21]. The higher the exchange rate in PT, the faster the convergence to the target distribution, and an algorithm is proposed in the limit where the exchange rate is infinite [22].

BPS also suffers from slow convergence for complex target distributions. In this paper, we first introduced PT into BPS. Next, following Ref. [22], we provided the algorithm of BPS-PT for the infinite exchange rate and proposed a method to evaluate an upper bound of the event rate. Then, we confirmed through numerical simulations that BPS-PT is more useful for multimodal distributions than BPS. In contrast, when the target distribution is simple, the benefits of BPS-PT are small because the computation time becomes significantly longer. Since this situation is the same as for PT with a finite exchange rate, it is best to compare the KS test values between the BPS and BPS-PT samples to assess the need for PT and use BPS-PT if necessary. Since the increase in computation time is mainly due to the combination of particle exchanges, we have to reduce the number of inverse temperatures as much as possible to decrease computation time. An efficient setting of inverse temperatures and their decomposition to subsets are issues for the future.

## Acknowledgments

YS and KT were supported by KAKENHI No. 20H05776. KT was also supported by KAKENHI Nos. 20H05774, 23K10978, 25H01509, and a grant from Hagiwara Foundation of Japan.

## References

- [1] Sumio Watanabe. Algebraic geometry and statistical learning theory, volume 25. Cambridge university press, 2009.
- [2] Atsushi Machida, Takeshi Watanabe, Masaichiro Mizumaki, Kenji Nagata, and Masato Okada. Development of a bayesian inference method for the analysis of x-ray reflectivity data. Japanese Journal of Applied Physics, 63(1):017005, 2024.
- [3] Brandon S Coventry and Edward L Bartlett. Practical bayesian inference in neuroscience: Or how i learned to stop worrying and embrace the distribution. Eneuro, 11(7), 2024.
- [4] Gael M Martin, David T Frazier, Worapree Maneesoonthorn, Rubén Loaiza-Maya, Florian Huber, Gary Koop, John Maheu, Didier Nibbering, and Anastasios Panagiotelis. Bayesian forecasting in economics and finance: A modern review. International Journal of Forecasting, 40(2):811–839, 2024.
- [5] Laurent Valentin Jospin, Hamid Laga, Farid Boussaid, Wray Buntine, and Mohammed Bannamoun. Hands-on bayesian neural networks—a tutorial for deep learning users. IEEE Computational Intelligence Magazine, 17(2):29–48, 2022.
- [6] Christophe Andrieu and Johannes Thoms. A tutorial on adaptive mcmc. Statistics and computing, 18:343–373, 2008.

- [7] Peter J Rossky, Jimmie D Doll, and Harold L Friedman. Brownian dynamics as smart monte carlo simulation. The Journal of Chemical Physics, 69(10):4628–4633, 1978.
- [8] Radford M Neal et al. Mcmc using hamiltonian dynamics. Handbook of markov chain monte carlo, 2(11):2, 2011.
- [9] Guangyao Zhou. Mixed hamiltonian monte carlo for mixed discrete and continuous variables. Advances in Neural Information Processing Systems, 33:17094–17104, 2020.
- [10] Guangyao Zhou. Metropolis augmented hamiltonian monte carlo. arXiv preprint arXiv:2201.08044, 2022.
- [11] Elias AJF Peters and G de With. Rejection-free monte carlo sampling for general potentials. Physical Review E—Statistical, Nonlinear, and Soft Matter Physics, 85(2):026703, 2012.
- [12] Alexandre Bouchard-Côté, Sebastian J Vollmer, and Arnaud Doucet. The bouncy particle sampler: A non-reversible rejection-free markov chain monte carlo method. Journal of the American Statistical Association, 113(522):855–867, 2018.
- [13] George Deligiannidis, Daniel Paulin, Alexandre Bouchard-Côté, and Arnaud Doucet. Randomized hamiltonian monte carlo as scaling limit of the bouncy particle sampler and dimension-free convergence rates. The Annals of Applied Probability, 31(6):2612–2662, 2021.
- [14] Andrew Chin and Akihiko Nishimura. Mcmc using bouncy hamiltonian dynamics: A unifying framework for hamiltonian monte carlo and piecewise deterministic markov process samplers. arXiv preprint arXiv:2405.08290, 2024.
- [15] Chris Sherlock and Alexandre H Thiery. A discrete bouncy particle sampler. Biometrika, 109(2):335–349, 2022.
- [16] Paul Fearnhead, Sebastiano Grazi, Chris Nemeth, and Gareth O Roberts. Stochastic gradient piecewise deterministic monte carlo samplers. arXiv preprint arXiv:2406.19051, 2024.
- [17] Ethan Goan and Clinton Fookes. Stochastic bouncy particle sampler for bayesian neural networks. Stochastic Bouncy Particle Sampler for Bayesian Neural Networks, 2021.
- [18] Andrea Bertazzi, Dario Shariatian, Umut Simsekli, Eric Moulines, and Alain Durmus. Piecewise deterministic generative models. Advances in Neural Information Processing Systems, 37:93336–93373, 2024.
- [19] Alexandre Bouchard-Côté, Sebastian J. Vollmer, and Arnaud Doucet. The bouncy particle sampler: A non-reversible rejection-free markov chain monte carlo method. arXiv preprint arXiv:1510.02451.v1, 2017.
- [20] Robert H Swendsen and Jian-Sheng Wang. Replica monte carlo simulation of spin-glasses. Physical review letters, 57(21):2607, 1986.
- [21] Radford M Neal. Sampling from multimodal distributions using tempered transitions. Statistics and computing, 6:353–366, 1996.
- [22] Paul Dupuis, Yufei Liu, Nuria Plattner, and Jimmie D Doll. On the infinite swapping limit for parallel tempering. Multiscale Modeling & Simulation, 10(3):986–1022, 2012.
- [23] Radford M Neal. Monte carlo implementation. Bayesian learning for neural networks, pages 55–98, 1996.
- [24] Matthew D Hoffman, Andrew Gelman, et al. The no-u-turn sampler: adaptively setting path lengths in hamiltonian monte carlo. J. Mach. Learn. Res., 15(1):1593–1623, 2014.
- [25] PA W Lewis and Gerald S Shedler. Simulation of nonhomogeneous poisson processes by thinning. Naval research logistics quarterly, 26(3):403–413, 1979.
- [26] Charles J Geyer. Introduction to markov chain monte carlo. Handbook of markov chain monte carlo, 20116022(45):22, 2011.
- [27] Radford M Neal. Non-reversibly updating a uniform  $[0, 1]$  value for metropolis accept/reject decisions. arXiv preprint arXiv:2001.11950, 2020.
- [28] Hidemaro Suwa and Synge Todo. Markov chain monte carlo method without detailed balance. Physical review letters, 105(12):120603, 2010.